Characterization of the Genomically Encoded Fosfomycin Resistance Enzyme from *Mycobacterium abscessus*

Journal:	*RSC Medicinal Chemistry*
Manuscript ID	MD-RES-07-2019-000372.R1
Article Type:	Research Article
Date Submitted by the Author:	31-Aug-2019
Complete List of Authors:	Travis, Skye; University of Alabama, Chemistry & Biochemistry Shay, Madeline; University of Alabama, Chemistry & Biochemistry Manabe, Shino; RIKEN, Gilbert, Nathan; Louisiana State University, Center for Advanced Microstructures and Devices Frantom, Patrick; University of Alabama, Chemistry & Biochemistry Thompson, Matthew; University of Alabama, Chemistry & Biochemistry

Characterization of the Genomically Encoded Fosfomycin Resistance Enzyme from Mycobacterium abscessus

Skye Travis[1†], Madeline R. Shay[1†], Shino Manabe[2], Nathaniel C. Gilbert[3], Patrick Frantom[1], Matthew K. Thompson[1*]

1. Department of Chemistry & Biochemistry, The University of Alabama, 250 Hackberry Lane, Tuscaloosa AL 35487
2. Synthetic Cellular Chemistry Laboratory, RIKEN, Hirosawa, Wako, Saitama 351-0198, Japan
3. Center for Advanced Microstructures and Devices, Louisiana State University, 6980 Jefferson Highway, Baton Rouge, Louisiana, 70806

†Denotes equal contribution.
*To whom correspondence should be addressed.
Matthew K. Thompson
Department of Chemistry & Biochemistry
The University of Alabama
Box 870336
Tuscaloosa AL 35487
Email: mthompson10@ua.edu
Phone: (205) 348-7020

Abstract

Mycobacterium abscessus belongs to a group of rapidly growing mycobacteria (RGM) and accounts for approximately 65-80% of lung disease caused by RGM. It is highly pathogenic and is considered the prominent Mycobacterium involved in pulmonary infection in patients with cystic fibrosis and chronic pulmonary disease (CPD). FosM is a putative 134 amino acid fosfomycin resistance enzyme from M. abscessus subsp. bolletii that shares approximately 30-55% sequence identity with other Vicinal Oxygen Chelate (VOC) fosfomycin resistance enzymes and represents the first of its type found in any Mycobacterium species. Genes encoding VOC fosfomycin resistance enzymes have been found in both Gram-positive and Gram-negative pathogens. Given that FosA enzymes from Gram-negative bacteria have evolved optimum activity towards glutathione (GSH) and FosB enzymes from Gram-positive bacteria have evolved optimum activity towards bacillithiol (BSH), it was originally suggested that FosM might represent a fourth class of enzyme that

has evolved to utilize mycothiol (MSH). However, a sequence similarity network (SSN) analysis identifies FosM as a member of the FosX subfamily, indicating that it may utilize water as a substrate. Here we have synthesized MSH and characterized FosM with respect to divalent metal ion activation and nucleophile selectivity. Our results indicate that FosM is a Mn^{2+}-dependent FosX-type hydrase with no selectivity toward MSH or other thiols as analyzed by NMR and mass spectroscopy.

Introduction

Mycobacterium abscessus is a rapidly growing mycobacterium (RGM) that has acquired recognition as a significant human pathogen responsible for a wide spectrum of soft tissue infections, infections in immunocompromised patients, and a contraindication to lung transplantation.[1-3] M. abscessus subsp. bolletii was first isolated in 2006 from patients with chronic pneumonia and cystic fibrosis.[4] It is highly pathogenic and is an increasing cause of human pulmonary disease and infections of the skin and soft tissue.[2, 3] It is now considered the prominent Mycobacterium in pulmonary infections associated with cystic fibrosis and chronic pulmonary disease (CPD).[5, 6] Clinical outbreaks of M. abscessus have been reported and demonstrate the organism's importance in hospital-acquired infections (HAIs).[7-9] The major threat posed by M. abscessus is due to its extensive resistance to current antibiotics, including clarithromycin, the antibiotic of choice for treating respiratory infections.[4, 10] Herein, we characterize the enzymatic resistance mechanism of M. abscessus to the antibiotic fosfomycin.

Fosfomycin, or (1R, 2S)-epoxypropylphosphonic acid (**Figure 1**) is a safe broad-spectrum antibiotic.[11] It was initially characterized in 1969 and has been used in several European countries for many years.[12] The United States Food and Drug Administration approved fosfomycin in 1996 for the treatment of uncomplicated urinary tract and gastrointestinal infections.[13, 14] It is effective against both Gram-positive and Gram-negative bacteria owing to its ability to inhibit cell wall biosynthesis by irreversibly inactivating the enzyme UDP-N-acetylglucosamine-3-enolpyruvyltransferase (MurA).[15-17] It has a low molecular weight and a relatively long half-life (5.7 ± 2.8 hrs),[18] which allows it to penetrate various tissues with ease and achieve the MICs necessary to inhibit growth of most pathogens. Recently, fosfomycin has gained interest as an agent active against a range of multi-drug resistant (MDR) and extensively drug resistant (XDR) bacteria,[13, 19-21] and it has

been evaluated clinically for therapeutic potential by inhalation in patients with pulmonary infections associated with cystic fibrosis.[22, 23]

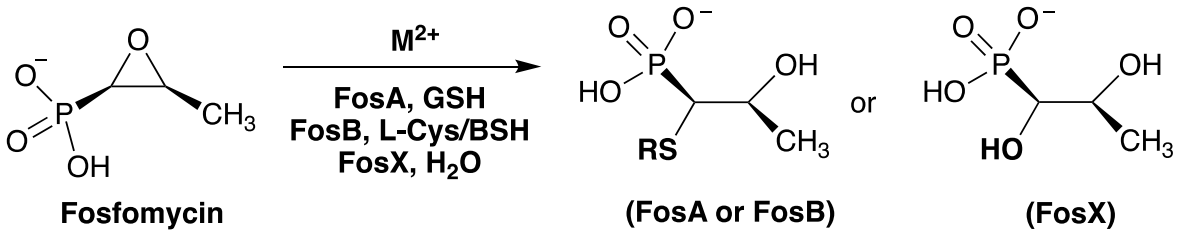

Figure 1. Reactions catalyzed by fosfomycin resistance enzymes.

There are currently three distinct classes of fosfomycin resistance enzymes belonging to the Vicinal Oxygen Chelate (VOC) superfamily (**Figure 1**). FosA enzymes are Mn^{2+}- and K^{+}-dependent glutathione-S-transferases that catalyze nucleophilic addition of glutathione (GSH) to fosfomycin resulting in a modified compound with no bactericidal properties.[24-27] FosA was initially discovered as a plasmid-borne resistance gene isolated from clinical samples of Serratia marcescens.[28] Later, genes encoding FosA were identified in several Gram-negative bacterial species including the opportunistic human pathogen Pseudomonas aeruginosa.[29] FosB enzymes were discovered in Gram-positive organisms such as Staphylococcus aureus and Bacillus anthracis.[30-32] They catalyze the Mn^{2+}-dependent addition of L-cysteine (L-Cys) or bacillithiol (BSH) to fosfomycin.[32, 33] FosX enzymes are Mn^{2+}-dependent hydrases that catalyze hydration of fosfomycin to inactivate the antibiotic.[34, 35] Genes encoding FosX have been found in numerous Gram-negative and Gram-positive bacterial species including Mesorhizobium loti, Mesorhizobium japonicum, Listeria monocytogenes, and Clostridium botulinum.[34, 35] However, the FosX enzymes perform the hydrase reaction with reduced catalytic efficiencies compared to FosA and FosB, and as a result, they are not considered to confer the same robust resistance to fosfomycin. For this reason, the FosX enzymes have been proposed to be evolutionary precursors to the more efficient fosfomycin resistance enzymes.[35, 36]

The complete genome of M. abscessus subsp. bolletii was reported in March 2012.[37] Within the genome, a gene encoding a putative fosfomycin resistance enzyme belonging to the VOC superfamily has been identified in Mycobacterium abscessus. The enzyme was named $FosM^{Mb}$ since it is the first of its type found in any Mycobacterium species.[38] Gram-negative bacteria, Gram-positive bacteria, and Mycobacteria have each evolved a different thiol: glutathione (GSH), bacillithiol (BSH), and mycothiol (MSH), respectively (**Figure 2**). Each different low-molecular-weight thiol serves the same function, to maintain cellular redox homeostasis and detoxify xenobiotic compounds from the organism. Just as the FosA enzymes from Gram-negative bacteria have evolved optimum activity towards GSH and the FosB enzymes from Gram-positive bacteria have evolved optimum activity towards BSH, it was originally suggested that $FosM^{Mb}$ might be a fourth class of fosfomycin resistance enzyme that has evolved to utilize MSH.[38] In this work, we use a sequence similarity network to visualize how the currently characterized VOC fosfomycin resistance enzymes are related to FosM within their taxonomic phyla. The sequence similarity results identify FosM as belonging to the FosX subfamily of the VOC superfamily. Moreover, we have synthesized MSH and subsequently characterized FosM with respect to metal activation and nucleophile selectivity. Our results indicate that FosM is a Mn^{2+}-dependent FosX-type hydrase with no selectivity toward MSH or other thiols as analyzed by NMR and mass spectroscopy.

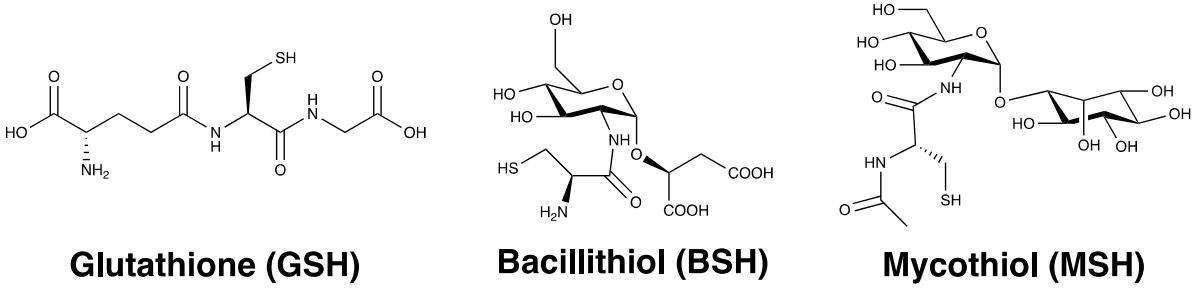

Figure 2. Structures of low molecular weight thiols found in Gram-negative bacteria, Gram-positive bacteria, and Mycobacteria. Gram-negative bacteria biosynthesis GSH, Gram-positive bacteria biosynthesize BSH, and Mycobacteria biosynthesize MSH.

Results and Discussion

FosM^{Mb} is a putative 134 amino acid fosfomycin resistance enzyme from M. abscessus subsp. bolletii that shares approximately 30% sequence identity with FosA and FosB, as well as 55% identity with FosX. Furthermore, FosM contains nearly every amino acid found in the active site of FosA, FosB, or FosX (**Figure 3**). Residues from FosM that coordinate the catalytically important divalent metal are His6, His68, and Glu117. These three metal coordinating ligands are tightly conserved throughout the VOC superfamily of fosfomycin resistance enzymes. Moreover, the most important residues that form a hydrogen-bonding network to fosfomycin are also conserved. Fosfomycin is a polar small molecule with both hydrophobic and hydrophilic ends. Other VOC fosfomycin resistance enzymes have evolved a hydrogen bond "cage" around the antibiotic.[32] The polar phosphonate group of the molecule is typically coordinated by two arginines and two tyrosines. These residues are conserved in FosM as Arg96, Arg126, Tyr66, and Tyr107. On the other side of the active site, the methyl group of fosfomycin is directly adjacent to an aromatic tryptophan. This residue is also conserved in FosM as Trp52. Thus, every residue that interacts with the metal or fosfomycin in other VOC fosfomycin resistance enzymes is found in FosM.

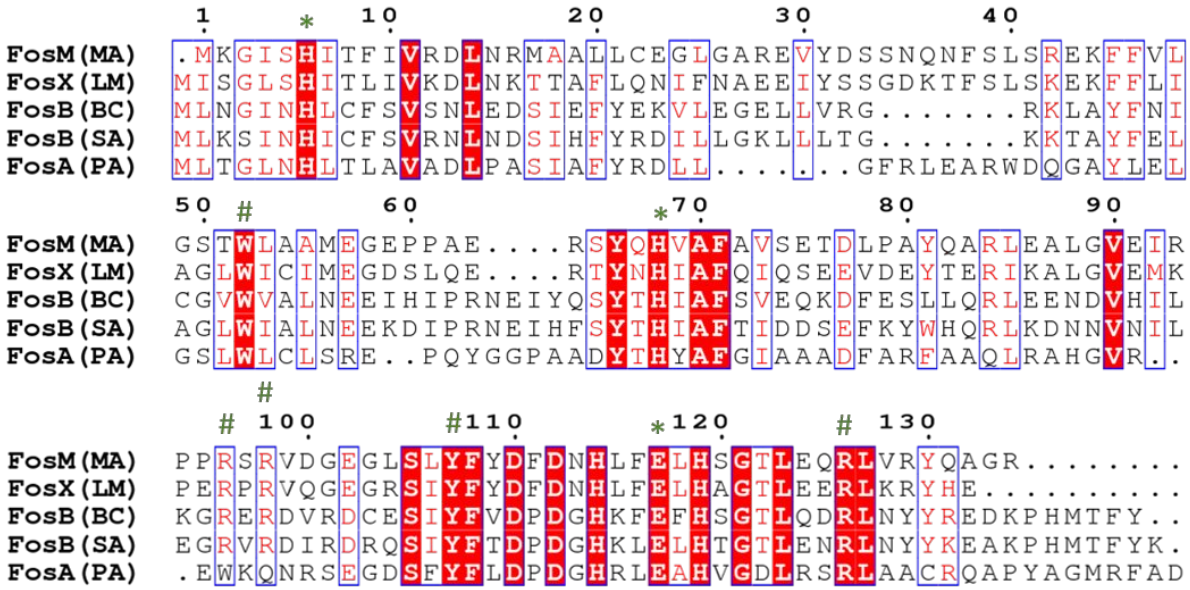

Figure 3. Sequence alignment of fosfomycin resistance enzymes. Alignment was performed on the sequences of FosM from Mycobacterium abscessus, FosX from Listeria monocytogenes, FosB from Bacillus cereus, FosB from Staphylococcus aureus, and FosA from Pseudomonas aeruginosa. Residues marked with (*) are residues used in binding metals in the active site. Residues marked with (#) are residues important in coordinating fosfomycin. Red blocks depict residues that are conserved throughout all sequences. Blue boxes and red text depict residues or motifs that are highly, but not universally, conserved.

Analysis of the sequence alignment suggests that FosM belongs to the VOC superfamily along with FosA, FosB, and FosX enzymes. Within the superfamily however, FosM is found in a subfamily of sequences categorized as "Fosfomycin resistance proteins, FosX" by the InterPro database (IPR037434). This subfamily contains 229 sequences including two Swiss-Prot annotated sequences corresponding to FosX (Uniprot IDs Q8Y612 and Q98GG1) and the recently discovered FosM, but it does not contain entries for FosA or FosB. To visualize the sequence landscape of the FosX/M subfamily, a sequence similarity network (SSN) was constructed using sequences from the IPR037434 accession number in the InterPro database using the Enzyme Function Initiative – Enzyme Similarity Tool[39] (**Figure 4**). SSNs are useful tools for the rapid visualization of results from an all-vs-all BLAST analysis of a database of sequences.[40] Each node represents a specific sequence and an edge is drawn between two nodes if their E-value meets a certain threshold. As the threshold is made more stringent, fewer edges are drawn and clusters of sequences develop. The program Cytoscape[41] can then be used to map orthogonal data onto the network. In **Figure 4**, a series of networks are shown with increasingly stringent E-value cutoffs (**4A**, 10^{-45} or lower; **4B**, 10^{-50} or lower; and **4C**, 10^{-55} or lower). Nodes are colored by taxonomic phylum for each sequence.

The majority of the sequences in this family are found in either the Firmicutes (Gram-positive organisms, green nodes) or Proteobacteria (Gram-negative organisms, orange nodes) phyla. Nodes for the two characterized members of this family (FosX from M. japonicum and L. monocytogenes), along with FosM from M. abscessus, are shown in bold on each network.

Figure 4C shows the network resolves to several mono-phylum clusters and one multi-phyla cluster containing sequences from Proteobacteria, Firmicutes, and Cyanobacteria. This multi-phyla cluster contains FosX from M. japonicum, a Gram-negative organism. The two mono-phylum Firmicute clusters contain one cluster represented by the characterized FosX from L. monocytogenes with the other cluster formed by sequences from the Clostridia and Bacilli classes. The cluster containing FosM is primarily made up of organisms from the Proteobacteria phylum with FosM as the sole representative of the Actinobacteria. As Gram-negative organisms, Proteobacteria likely utilize GSH as their preferred reductant. Therefore, the other organisms in the FosM-containing cluster are not expected to produce MSH. We investigated whether the putative FosM enzyme is a hydrase, a GSH transferase, or a MSH transferase.

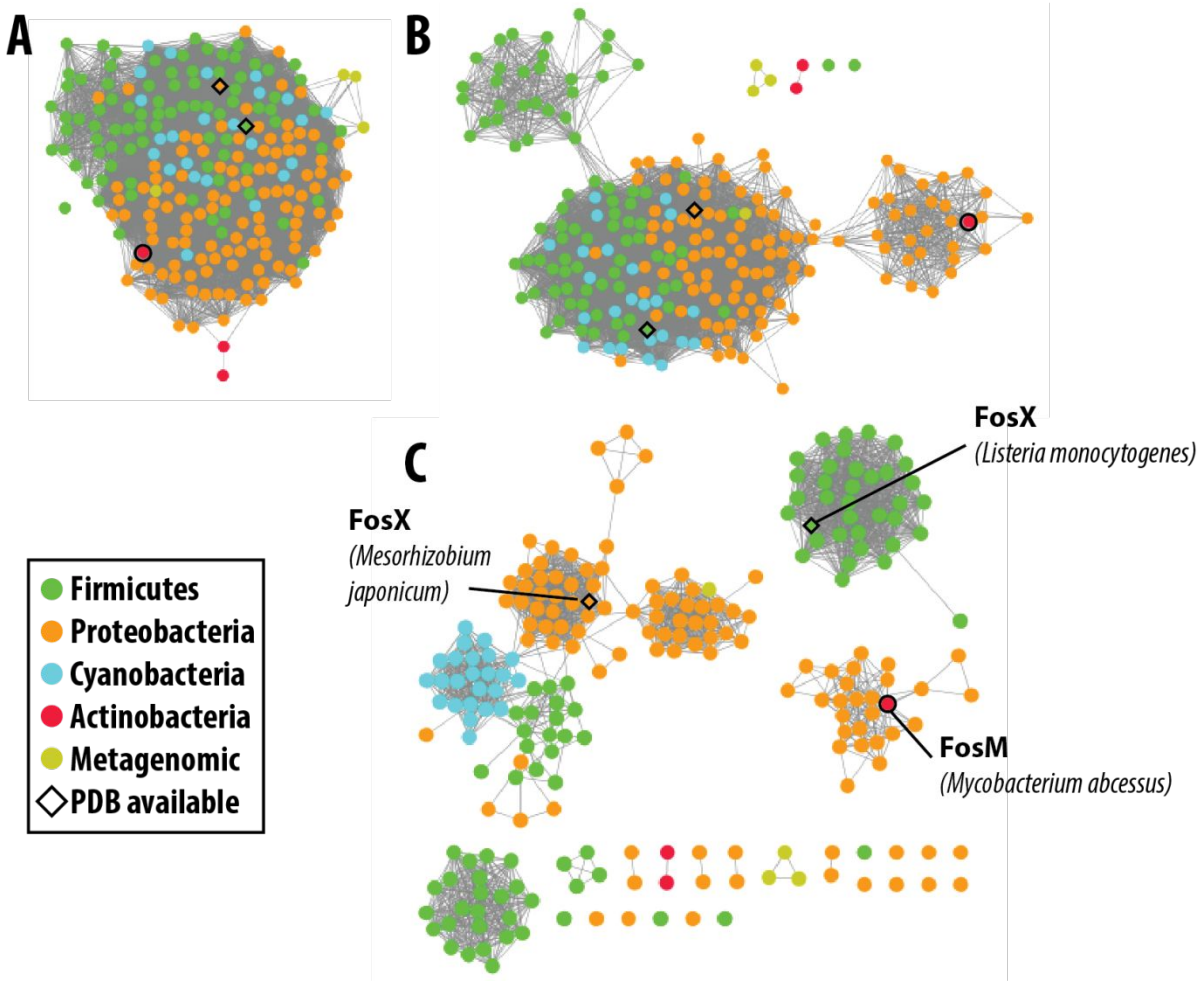

Figure 4. Sequence similarity networks of the IPR037434 family. The sequence similarity networks were visualized using Cytoscape as described in materials and methods. To visualize how the clusters develop, networks constructed at alignment score cutoff of 10^{-45} (A), 10^{-50} (B), and 10^{-55} (C) are shown. Nodes are colored by taxonomic phylum as described in the legend. Nodes with a diamond shape have structural data reported in the PDB databank. The network in panel C has 223 nodes and 2066 edges with an average of 84% sequence identity over 135 residues.

We have expressed FosM in E. coli and developed a purification protocol that results in homogenous, stable protein at >95% purity for biochemical characterization (**Figure S1**). Members of the VOC fosfomycin resistance enzymes are a superfamily of metalloenzymes characterized by a 3D domain-swapped arrangement of tandem βαβββ motifs.[29, 32, 34, 42, 43] We used circular dichroism (CD) spectroscopy to investigate the secondary structure of FosM (**Figure 5**). Foremost, the CD spectrum of FosM indicates that the expressed protein is folded in solution. Comparative analysis of FosM from M. abscessus, FosA from P. aeruginosa, FosB from B. cereus and FosX from L. monocytogenes indicates that the secondary structure of FosM is slightly different from the representative FosA, FosB, and FosX proteins. We used an online analysis tool for protein CD spectra, DichroWeb,[44] to estimate percent secondary structure composition for each protein. Results from the DichroWeb analysis are summarized in **Table 1**. **Figure S2** shows the calculated fits for each of the experimental CD spectra.

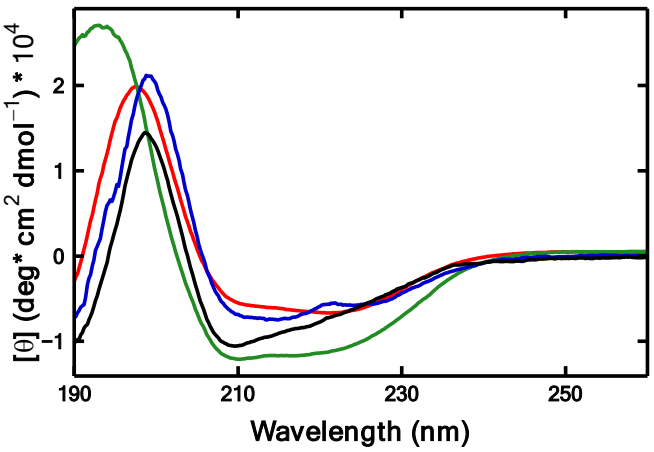

Figure 5. Circular dichroism (CD) spectra of the fosfomycin resistance enzymes, FosA from P. aeruginosa, FosB from B. cereus, FosX from L. monocytogenes, and FosM from M. abscessus. The proteins were stored in 20mM HEPES pH 7.0, and diluted in MQ water for

the scan. The distinct secondary structure of FosM (black) is richer in β-sheet character than that shown for FosA (green) and FosX (red) enzymes as indicated by the relatively sharper peak at ~210 nm.

The estimated secondary structure composition for FosM suggests more β-sheet characteristics than the representative FosA and FosX enzymes. In fact, the estimated α-helix and β-sheet contents are most similar to that of FosB. This was a somewhat unanticipated result given that FosM shares 55% sequence similarity with FosX and only 30% with either FosA or FosB. Nevertheless, the results are consistent with the typically βαβββ motif. Interestingly, the secondary structure analysis also indicates a relatively equivalent amount of "disordered" characteristic across all the evaluated CD spectra. This is consistent with the proposed mechanism of the VOC fosfomycin enzymes. There are two structurally dynamic loop regions of the enzymes that are believed to be in an unfolded, "open" configuration to allow fosfomycin access to the active site. The loop regions then "close" around the antibiotic to form the nucleophile-binding site.[42] Binding studies of FosB have indicated the antibiotic must bind first followed by nucleophilic attack of the cosubstrate.[45] The greater structural similarity of FosM to FosB suggested that FosM might use a different mechanism than FosX, where MSH is utililized as the cosubstrate.

Table 1. Percent Secondary Structure.

Metal	$FosM^{Mb}$	$FosX^{LM}$	$FosB^{BC}$	$FosA^{PS}$
α-helix	0.21	0.35	0.18	0.54
β-sheet	0.36	0.23	0.42	0.23
Turn	0.20	0.20	0.16	0.06
Disordered	0.23	0.22	0.23	0.17
Total	1.00	1.00	0.99	1.00
nrmsd*	0.012	0.023	0.019	0.002

To investigate the nucleophilic selectivity of FosM, we conducted endpoint assays and analyzed the products by mass spectroscopy. Reactions were carried out in the presence of water only, L-Cys, GSH, and MSH (**Figure 6**). We use L-Cys as a BSH analog given that

all of the FosB enzymes characterized to date can catalyze nucleophilic addition of L-Cys to fosfomycin. **Figure 6A** shows the fosfomycin standard (no enzyme added) with a mass of 136.9998 as expected. **Figure 6B** shows the same conditions in the presence of FosM. Here, the mass for fosfomycin is completely absent and a new mass at 155.0120 is observed corresponding to the addition of water to the antibiotic. **Figures 6C** and **6D** show results for the reactions with L-Cys and GSH, respectively. For either of these reactions, only the hydrated fosfomycin product is observed, and the masses for L-Cys and GSH, 120.0100 and 306.0732, respectively, are still present in the spectra. We note that the L-Cys mass appears suppressed in the spectrum. This occurred in every replicate we attempted, and no L-Cys fosfomycin product was ever observed.

To test the original hypothesis that FosM from M. abscessus might in fact be an MSH transferase, we repeated the reaction in the presence of MSH (**Figure 6E**). The mass at 485.1404 corresponds to MSH. Once again, only the hydrated fosfomycin product mass is observed, and no mass corresponding to the addition of MSH to fosfomycin is present in the product analysis. Other masses present in the sample can be attributed to impurities in the MSH sample left over from the synthesis. The results indicate that FosM from M. abscessus catalyzes hydration of fosfomycin and is not a thiol transferase.

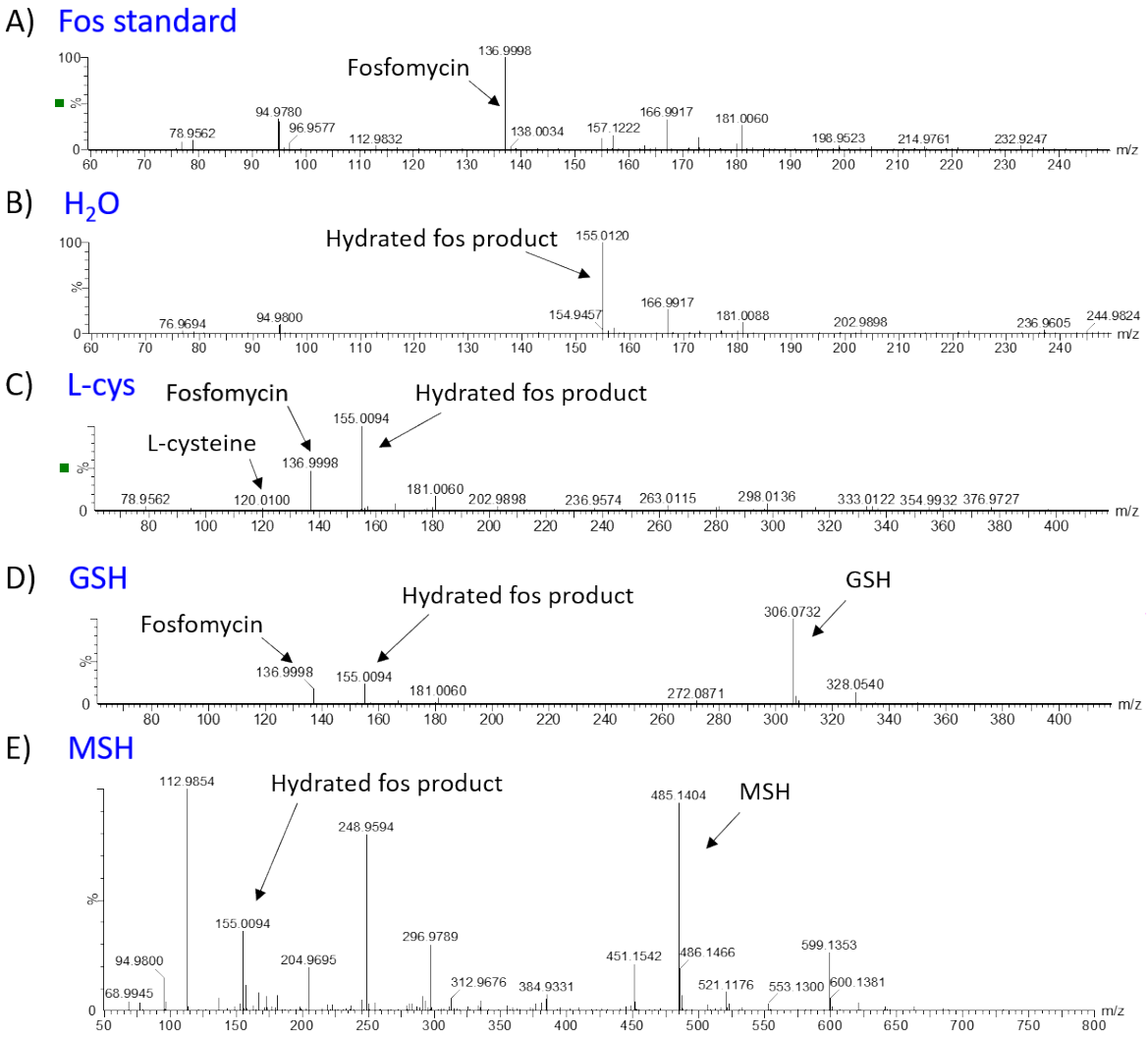

Figure 6. TOF MS ES data of FosM with various substrates and product. Reactions were carried out in water at 25°C with: 8 mM fosfomycin (A); 0.6 µM FosM and 8 mM fosfomycin (B); 0.6 µM FosM, 8 mM fosfomycin, and 4 mM L-Cys (C); 0.6 µM FosM, 8 mM fosfomycin, and 4 mM GSH (D); 0.6 µM FosM, 8 mM fosfomycin, and 4 mM MSH (E). Other masses present in (E) are due to residual impurities from the MSH synthesis.

Once the nucleophile was identified, we used ^{31}P-NMR to probe the metal activation of FosM. ^{31}P NMR can readily monitor both fosfomycin and the resulting fosfomycin-thiol or fosfomycin-diol product from the enzymatic reactions (**Figure S3**). The ^{31}P method is quick and convenient, but it is not sensitive enough to determine detailed kinetic parameters. Nevertheless, apparent k_{cat} values can be approximated; therefore, the ^{31}P-NMR assay provides a qualitative assessment of the metal ion selectivity. Reactions were carried out at

25°C in 20 mM HEPES (pH 7.5) with 8 mM fosfomycin and 0.6 μM FosM in the presence of 4 mM L-Cys, GSH, or MSH (**Figure 7**).

The divalent metal activation of FosA, FosB, and FosX has been reported.[26, 27, 30, 32, 34] In general, the VOC fosfomycin resistance enzymes are activated by Mn^{2+} and inhibited by Zn^{2+}, with limited activity in the presence of other divalent metal ions. The metal activation of FosM follows the same trend as other VOC fosfomycin resistance enzymes with $Mn^{2+} >> Zn^{2+} \approx Mg^{2+}$. Although Zn^{2+} does not inhibit FosM like the other VOC enzymes, it follows the same general activation trend. The apparent k_{cat} values for FosM and Mn^{2+}, Zn^{2+}, or Mg^{2+} are 15.1 s^{-1}, 0.7 s^{-1}, and 0.4 s^{-1}, respectively. In the absence of FosM, no fosfomycin-diol product was formed under otherwise identical conditions (**Figure S4**). This confirms FosM is a Mn^{2+}-dependent hydrase.

When activated by Mn^{2+}, the turnover number of FosM compares well with those of other kinetically characterized VOC fosfomycin resistance enzymes. The k_{cat} for FosX from L. monocytogenes is reported to be 34 s^{-1}, whereas the k_{cat} for FosX from M. loti is 0.15 s^{-1}, although $FosX^{Ml}$ is not expected to confer fosfomycin resistance.[35] The apparent k_{cat} values for FosB from B. cereus and FosB from S. aureus with BSH and Mn^{2+} are 26.7 and 5.98 s^{-1}, respectively.[32, 42] Finally, the k_{cat} for FosA from P. aeruginosa with GSH when activated my Mn^{2+} is 180 s^{-1}.[46] These values allows us to place the activity of FosM within similar context to the other VOC resistance enzymes. However, a hardline comparison is not appropriate since the assays were conducted using different techniques with different starting concentrations of the cosubstrates. Regardless, the comparison shows that FosM from M. abscessus is a viable fosfomycin resistance enzyme.

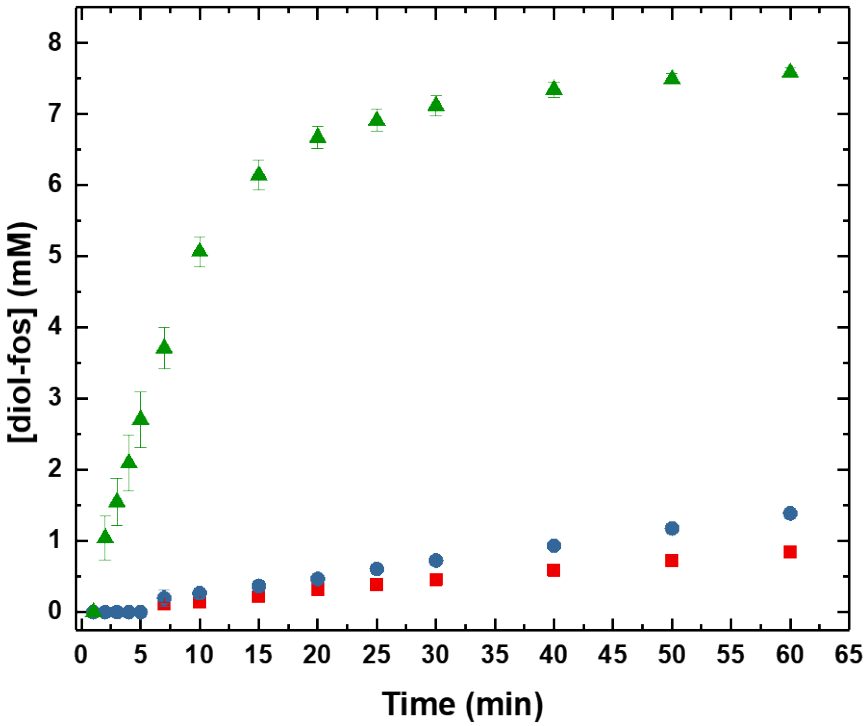

Figure 7. Time-trace kinetics for the FosM-catalyzed addition of water to fosfomycin in the presence of Mn^{2+} (▲), Mg^{2+} (■), or Zn^{2+} (●). Reactions were carried out at 25 °C with 8 mM fosfomycin and 0.6 μM enzyme in 20 mM HEPES, pH 7.5. In the absence of FosM, no hydrated fosfomycin product was formed under otherwise identical conditions (**Figure S4**).

After we determined that $FosM^{Mb}$ is a FosX-type hydrase, we made a structural homology model using FosX as the reference (**Figure 8**). Using the Modeller[47] extension of the Chimera program suite,[48] we threaded the FosM sequence onto FosX PDB entry 2P7O, the highest resolution and most complete FosX structure available. An overlay of the FosM, FosX, FosA and FosB active sites is very informative from a mechanistic perspective (**Figure 8**). There is a large degree of structural similarity between the four enzymes that extends beyond the metal binding ligands. The similarities include Thr8 in FosA and Thr9 in FosX, which are proposed to activate the oxirane oxygen of fosfomycin via proton donation to form the resulting product alcohol.[29, 35] Similarly for FosB, Cys9 has been proposed to activate the oxirane oxygen.[32] Moreover, for FosX, residue Glu44 has been shown to be critical for catalytic activity.[35] The structurally equivalent residue is Glu43 in FosM, Gly37 in FosA and Leu37 in FosB. The Glu44 residue in FosX serves as the primary component of the general base catalytic mechanism for direct addition of water to the antibiotic.[35] Mutation of the

residue nearly abolishes enzymatic activity in FosX from L. monocytogenes and M. loti. Both FosA and FosB utilize Tyr39 in their catalytic mechanisms to deprotonate the incoming nucleophilic thiol. Mutation of the residue to phenylalanine in FosA from P. aeruginosa results in a 13-fold reduction in enzymatic turnover.[49] Based on structural alignment of the FosM homology model with FosA and FosB, the structurally corresponding residue in FosX/M is, interestingly, a phenylalanine. Thus, one of the most important residues associated with thiol transferase activity found in FosA and FosB is absent in FosX/M, whereas one of the most important residues associated with hydrase activity is found in FosX/M and absent in FosA and FosB.

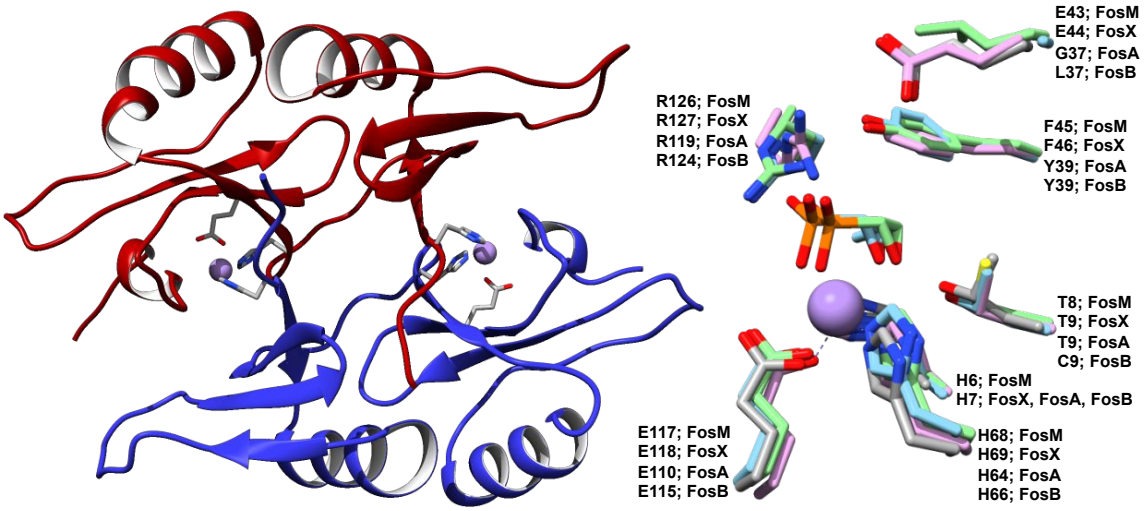

Figure 8. (Left) FosM homology model based on FosX with the two subunits illustrated in blue and red. The positions of the Mn^{2+} ions are shown in purple. This image was generated using the program Chimera (ref). (Right) Overlay of the active site residues of FosA (blue PDB entry 1LQP), FosB (green PDB entry 4JH6), FosX (purple; PDB entry 1R9C), and FosM (grey) with bound fosfomycin from FosA and FosB and Mn^{2+}.

Conclusion

We have characterized the recently discovered fosfomycin resistance enzyme, FosM, from M. abscessus. FosM belongs to the Vicinal Oxygen Chelate superfamily of fosfomycin resistance metalloenzymes and represents a FosX-type hydrase that utilizes a Mn^{2+}-dependent fosfomycin inactivation mechanism involving nucleophilic addition of water to the

antibiotic. With the rise of multidrug-resistance and extensively drug-resistant bacteria, discovery of new avenues and revitalization of approved, safe antibiotics like fosfomycin are of critical importance to combat antimicrobial resistance. Inhibition of the antibiotic-target-modifying enzyme FosM may prove an attractive approach to restoring the clinical effectiveness of fosfomycin as a treatment for upper respiratory infections. Ongoing efforts are being made to determine the 3-dimensional X-ray crystal structure of FosM and perform a full steady-state kinetic analysis of the enzyme in order to evaluate its true role in fosfomycin resistance.

Experimental

General Materials

Buffer salts were purchased from VWR. Metals were obtained as their chloride salts. Manganese (II) chloride was acquired from ACROS Organics. Magnesium chloride hexahydrate and Zinc chloride were purchased from Fisher Scientific. L-Cysteine was purchased from Fisher Chemical; glutathione was purchased from VWR. Fosfomycin disodium salt was from MP Biomedicals, LLC.

Mycothiol Synthesis

Mycothiol (MSH) was synthesized according to published procedures.[50] The mycothiol synthesis results in pyridine and trifluoroacetic (TFA) acid impurities from the final step. The NMR spectrum for the MSH sample used is provided in **Figure S5.** The primary impurity in our sample is TFA with a mass of 112.9854. The mass at 485.1404 corresponds to MSH. Once we determined that FosM was a hydrase, the MSH was used without further purification. Moreover, the hydrase kinetics were nearly identical even in the presence of the MSH sample, indicating that none of the impurities inhibited the enzyme (**Figure S6)**.

Protein Expression and Purification

A pET-20b expression plasmid containing the gene encoding non-tagged wild type (WT) FosM from M. abscessus was transformed into Escherichia coli BL21 (DE3) cells. The cells were plated on LB agar containing 80 μg/mL of ampicillin and incubated at 37 °C for approximately 16 h. Single colonies were isolated from the LB-agar plates and used to inoculate 2 mL of LB (Fisher Bioreagents) starter cultures (3 cultures for a total of 6 mL) containing 80 μg/mL of ampicillin. After approximately 8 h of incubation at 37°C with shaking, 1 mL of starter growth was used to inoculate 1 L of Terrific Broth containing 80 μg/mL of ampicillin (6 L total). The 1 L cultures were grown at 37 °C with shaking until the OD_{600} reached ~1 and then induced with 0.5 mM IPTG. Upon induction with IPTG, the temperature was reduced to 25°C, and the cells were allowed to grow for an additional 18 to 20 h. The cells were harvested by centrifugation at 8,000 X g for 10 min. The cell pellet was stored at -80°C.

The E. coli cell pellet containing overexpressed FosM was resuspended in 2 mL of lysis buffer per gram of cell pellet. Lysis buffer was comprised of 20 mM Tris HCl, pH 7.5. Lysozyme was added to the slurry at 1 mg/mL, and the mixture was stirred at 4 °C for 30 minutes, after which 5 mg of DNase was added. The slurry was then stirred at 4 °C for an additional 30 minutes. The mixture was sonicated to ensure complete lysing of cells, and the lysate was cleared by centrifugation at 20,000 X g for 20 min.

An ammonium sulfate precipitation was performed on the cleared lysate solution prior to any column purification. Fractions were precipitated at 10, 20, 30, 40, 50, 60, and 70% ammonium sulfate. According to SDS-PAGE, the 20 to 40% fraction contained the highest ratio of FosM to other proteins and was used for further purification. The protein was dialyzed overnight in 20 mM HEPES buffer (pH 7.0) to remove any residual lysis buffer or salt that could interfere with anion-exchange chromatography.

The dialyzed fraction was concentrated and loaded onto a GE Healthcare HiPrep DEAE FF 16/10 anion exchange column equilibrated with 20 mM HEPES (pH 7.0) using BioRad NGC FPLC equipped with a separate sample load pump. With an estimated pI of 5.80, FosM adheres to the DEAE material, and a purple hue can be seen on the column. The protein was eluted from the column over 20 column volumes using a gradient of 0−30% NaCl in the same loading buffer. Fractions were analyzed for purity by SDS-PAGE. The most pure fractions were collected, combined, and dialyzed overnight into 10 mM sodium phosphate (pH 7.0).

The protein, in 10 mM sodium phosphate buffer (pH 7.0), was subsequently loaded onto a 2.5 × 15 cm gravity hydroxyapatite column (BioRad, Hercules, CA). FosM does not adhere to the hydroxyapatite material, and the flow-through contains pure FosM. The flow-through was collected and analyzed for purity by SDS-PAGE (**Figure S1)**.

The purified FosM protein was prepared with Mn^{2+}, Mg^{2+}, and Zn^{2+} by dialyzing into 50 mM Bis-Tris (pH 6.0) with 5 mM EDTA and 2 mM 1,10-phenanthroline to remove all bound metals. The protein was then dialyzed into 20 mM HEPES buffer (pH 7.5) containing 200 μM of the respective divalent metal. After dialysis, the protein was concentrated and the concentration was determined using a Thermo Scientific NanoDrop One.

Circular Dichroism

FosA from P. aeruginosa, FosB from B. cereus, and FosX from L. monocytogenes were expressed and purified according to published procedures for use in CD analysis.[32] Each purified protein was then concentrated and stored in 20mM HEPES pH 7.0. The samples were filtered through a 0.2 μm filter and diluted to 0.2 mg/mL in MQ water before being analyzed. Triplicate spectra were collected for secondary structure analysis of each protein in the absence of fosfomycin. Each spectrum was composed of 5 accumulations from a wavelength scan on a JASCO J-1500 circular dichroism spectrometer.

Secondary Structure Analysis

The percent secondary structure was analyzed utilizing CDSSTR[51] through the online DichroWeb server.[44] Each spectrum was analyzed from 190-260nm using the expanded reference data set.[51] This reference data set provided the best models for the experimental data, as determined by the normalized RMSD values.

Mass Spectrometry

All samples were prepared in water with 8 mM fosfomycin, with the thiol samples additionally containing 4 mM L-Cys, GSH, or MSH. The reaction was initiated by the addition of 0.6 μM FosM and allowed to continue at 25°C overnight to ensure full product formation. Each reaction was then quenched with 500 μL chloroform to precipitate the enzyme out of solution. Samples were centrifuged to ensure full separation, and the aqueous layer was tested using TOF MS ES.

Continuous ^{31}P NMR Assays with Mn^{2+}, Zn^{2+} and Mg^{2+}

FosM was purified and prepared with 200 μM Mn^{2+}, Mg^{2+}, or Zn^{2+} bound for testing metal activation. 8 mM fosfomycin was prepared in 20 mM HEPES (pH 7.5) and the reaction was initiated by the addition of 0.6 μM FosM. The reaction was transferred to an NMR tube and allowed to continue at 25°C. The ratio of the concentration of fosfomycin to the concentration of the product was monitored continuously by obtaining spectra at various time points up to 60 minutes using a Bruker Avance 500 MHz NMR. The data were analyzed using Bruker TopSpin software.

Sequence Similarity Network Generation

A sequence similarity network[40] (SSN) was generated for the IPR037434 family in the InterPro database (version 72.0) using the Enzyme Function Initiative – Enzyme Similarity Tool[39] (EFI-EST) maintained by the Enzyme Function Initiative

(www.enzymefunction.org). All 228 sequences were used to generate the SSN. The resulting network was downloaded as a Cytoscape[41] readable xgmml file for visualization.

Acknowledgements

We would like to acknowledge The University of Alabama start-up funds for support of this project. S.T. would like to acknowledge the Department of Education GAANN Grant #P200A150329. M.S. would like to acknowledge The University of Alabama Undergraduate Creativity and Research Award. M.K.T would like to acknowledge the generosity of the Richard N. Armstrong family and Vanderbilt University Department of Biochemistry for initial laboratory equipment along with plasmids and reagents specific to this project. P.A.F. was supported by NSF CAREER Award (MCB-1254007).

Conflicts of Interest

There are no conflicts of interest to declare.

References

1. D. E. Griffith, T. Aksamit, B. A. Brown-Elliot, A. Catanzaro, C. Daley, F. Gordin, S. M. Holland, R. Horsburgh, G. Huitt, M. F. Iademarco, M. Iseman, K. Olivier, S. Ruoss, C. F. von Reyn, R. J. Wallace, Jr. and K. Winthrop, Am. J. Respir. Crit. Care Med., 2007, **175**, 367-416.
2. W.-J. Koh, O. J. Kwon, N. Y. Lee, Y.-H. Kook, H.-K. Lee and B.-J. Kim, J. Clin. Microbiol., 2009, **47**, 3362-3366.
3. A. M. Zelazny, J. M. Root, Y. R. Shea, R. E. Colombo, I. C. Shamputa, F. Stock, S. Conlan, S. McNulty, B. A. Brown-Elliott, R. J. Wallace, Jr., K. N. Olivier, S. M. Holland and E. P. Sampaio, J. Clin. Microbiol., 2009, **47**, 1985-1995.
4. T. Adekambi, P. Berger, D. Raoult and M. Drancourt, Int. J. Syst. Evol. Microbiol., 2006, **56**, 133-143.
5. D. E. Griffith, W. M. Girard and R. J. Wallace, Jr., Am Rev Respir Dis, 1993, **147**, 1271-1278.
6. I. Sermet-Gaudelus, B. M. Le, C. Pierre-Audigier, C. Offredo, D. Guillemot, S. Halley, C. Akoua-Koffi, V. Vincent, V. Sivadon-Tardy, A. Ferroni, P. Berche, P. Scheinmann, G. Lenoir and J.-L. Gaillard, Emerg Infect Dis, 2003, **9**, 1587-1591.
7. S. C. Leao, E. Tortoli, C. Viana-Niero, S. Y. M. Ueki, K. V. B. Lima, M. L. Lopes, J. Yubero, M. C. Menendez and M. J. Garcia, J. Clin. Microbiol., 2009, **47**, 2691-2698.
8. C. Viana-Niero, K. V. B. Lima, M. L. Lopes, M. C. d. S. Rabello, L. R. Marsola, V. C. R. Brilhante, A. M. Durham and S. C. Leao, J. Clin. Microbiol., 2008, **46**, 850-855.
9. R. J. Wallace, Jr., B. A. Brown and D. E. Griffith, Annu. Rev. Microbiol., 1998, **52**, 453-490.
10. T. Adekambi and M. Drancourt, Emerging Infect. Dis., 2009, **15**, 302-305.
11. A. C. Dijkmans, N. V. O. Zacarías, J. Burggraaf, J. W. Mouton, E. B. Wilms, C. van Nieuwkoop, D. J. Touw, J. Stevens and I. M. C. Kamerling, Antibiotics (Basel, Switzerland), 2017, **6**, 24.
12. D. Hendlin and a. et, Science, 1969, **166**, 122-123.
13. M. E. Falagas, K. P. Giannopoulou, G. N. Kokolakis and P. I. Rafailidis, Clin Infect Dis, 2008, **46**, 1069-1077.
14. M. E. Falagas, A. C. Kastoris, D. E. Karageorgopoulos and P. I. Rafailidis, Int. J. Antimicrob. Agents, 2009, **34**, 111-120.
15. S. Eschenburg, W. Kabsch, M. L. Healy and E. Schoenbrunn, J. Biol. Chem., 2003, **278**, 49215-49222.
16. S. Eschenburg, M. Priestman and E. Schoenbrunn, J. Biol. Chem., 2005, **280**, 3757-3763.
17. S. Eschenburg, M. A. Priestman, F. A. Abdul-Latif, C. Delachaume, F. Fassy and E. Schoenbrunn, J. Biol. Chem., 2005, **280**, 14070-14075.
18. S. S. Patel, J. A. Balfour and H. M. Bryson, Drugs, 1997, **53**, 637-656.
19. M. E. Falagas, A. P. Grammatikos and A. Michalopoulos, Expert Rev Anti Infect Ther, 2008, **6**, 593-600.
20. M. E. Falagas, A. C. Kastoris, A. M. Kapaskelis and D. E. Karageorgopoulos, Lancet Infect. Dis., 2010, **10**, 43-50.
21. M. E. Falagas, S. Maraki, D. E. Karageorgopoulos, A. C. Kastoris, E. Mavromanolakis and G. Samonis, Int. J. Antimicrob. Agents, 2010, **35**, 240-243.
22. M. E. Falagas, E. K. Vouloumanou, A. G. Togias, M. Karadima, A. M. Kapaskelis, P. I. Rafailidis and S. Athanasiou, J. Antimicrob. Chemother., 2010, **65**, 1862-1877.

23. B. C. Trapnell, S. A. McColley, D. G. Kissner, M. W. Rolfe, J. M. Rosen, M. McKevitt, L. Moorehead, A. B. Montgomery and D. E. Geller, Am. J. Respir. Crit. Care Med., 2012, **185**, 171-178.
24. P. Arca, C. Hardisson and J. E. Suarez, Antimicrob. Agents Chemother., 1990, **34**, 844-848.
25. P. Arca, M. Rico, A. F. Brana, C. J. Villar, C. Hardisson and J. E. Suarez, Antimicrob. Agents Chemother., 1988, **32**, 1552-1556.
26. B. A. Bernat, L. T. Laughlin and R. N. Armstrong, Biochemistry, 1997, **36**, 3050-3055.
27. B. A. Bernat, L. T. Laughlin and R. N. Armstrong, Biochemistry, 1999, **38**, 7462-7469.
28. J. M. Garcia-Lobo and J. M. Ortiz, J. Bacteriol., 1982, **151**, 477-479.
29. C. L. Rife, R. E. Pharris, M. E. Newcomer and R. N. Armstrong, J. Am. Chem. Soc., 2002, **124**, 11001-11003.
30. M. Cao, B. A. Bernat, Z. Wang, R. N. Armstrong and J. D. Helmann, J. Bacteriol., 2001, **183**, 2380-2383.
31. R. E. Rigsby, K. L. Fillgrove, L. A. Beihoffer and R. N. Armstrong, Methods Enzymol., 2005, **401**, 367-379.
32. M. K. Thompson, M. E. Keithly, J. Harp, P. D. Cook, K. L. Jagessar, G. A. Sulikowski and R. N. Armstrong, Biochemistry, 2013, **52**, 7350-7362.
33. A. P. Lamers, M. E. Keithly, K. Kim, P. D. Cook, D. F. Stec, K. M. Hines, G. A. Sulikowski and R. N. Armstrong, Org. Lett., 2012, **14**, 5207-5209.
34. K. L. Fillgrove, S. Pakhomova, M. R. Schaab, M. E. Newcomer and R. N. Armstrong, Biochemistry, 2007, **46**, 8110-8120.
35. K. L. Fillgrove, S. Pakhomova, M. E. Newcomer and R. N. Armstrong, J. Am. Chem. Soc., 2003, **125**, 15730-15731.
36. P. J. O'Brien and D. Herschlag, Chem Biol, 1999, **6**, R91-R105.
37. G.-E. Choi, Y.-J. Cho, W.-J. Koh, J. Chun, S.-N. Cho and S. J. Shin, J. Bacteriol., 2012, **194**, 2756-2757.
38. M. K. Thompson, M. E. Keithly, G. A. Sulikowski and R. N. Armstrong, Perspectives in Science, 2015, **4**, 17-23.
39. J. A. Gerlt, J. T. Bouvier, D. B. Davidson, H. J. Imker, B. Sadkhin, D. R. Slater and K. L. Whalen, Biochimica et Biophysica Acta, 2015, **1854**, 1019-1037.
40. H. J. Atkinson, J. H. Morris, T. E. Ferrin and P. C. Babbitt, PloS One, 2009, **4**, e4345-e4345.
41. P. Shannon, A. Markiel, O. Ozier, N. S. Baliga, J. T. Wang, D. Ramage, N. Amin, B. Schwikowski and T. Ideker, Genome Research, 2003, **13**, 2498-2504.
42. M. K. Thompson, M. E. Keithly, M. C. Goodman, N. D. Hammer, P. D. Cook, K. L. Jagessar, J. Harp, E. P. Skaar and R. N. Armstrong, Biochemistry, 2014, **53**, 755-765.
43. S. Pakhomova, C. L. Rife, R. N. Armstrong and M. E. Newcomer, Protein Sci., 2004, **13**, 1260-1265.
44. L. Whitmore and B. A. Wallace, Biopolymers, 2008, **89**, 392-400.
45. A. A. Roberts, S. V. Sharma, A. W. Strankman, S. R. Duran, M. Rawat and C. J. Hamilton, Biochem. J., 2013, **451**, 69-79.
46. D. W. Brown, M. R. Schaab, W. R. Birmingham and R. N. Armstrong, Biochemistry, 2009, **48**, 1847-1849.
47. A. Sali and T. L. Blundell, J Mol Biol, 1993, **234**, 779-815.

48. E. F. Pettersen, T. D. Goddard, C. C. Huang, G. S. Couch, D. M. Greenblatt, E. C. Meng and T. E. Ferrin, J. Comput. Chem., 2004, **25**, 1605-1612.
49. R. E. Rigsby, D. W. Brown, E. Dawson, T. P. Lybrand and R. N. Armstrong, Arch. Biochem. Biophys., 2007, **464**, 277-283.
50. S. Manabe and Y. Ito, Beilstein J. Org. Chem., 2016, **12**, 328-333.
51. N. Sreerama and R. W. Woody, Anal. Biochem., 2000, **287**, 252-260.

TOC Graphic

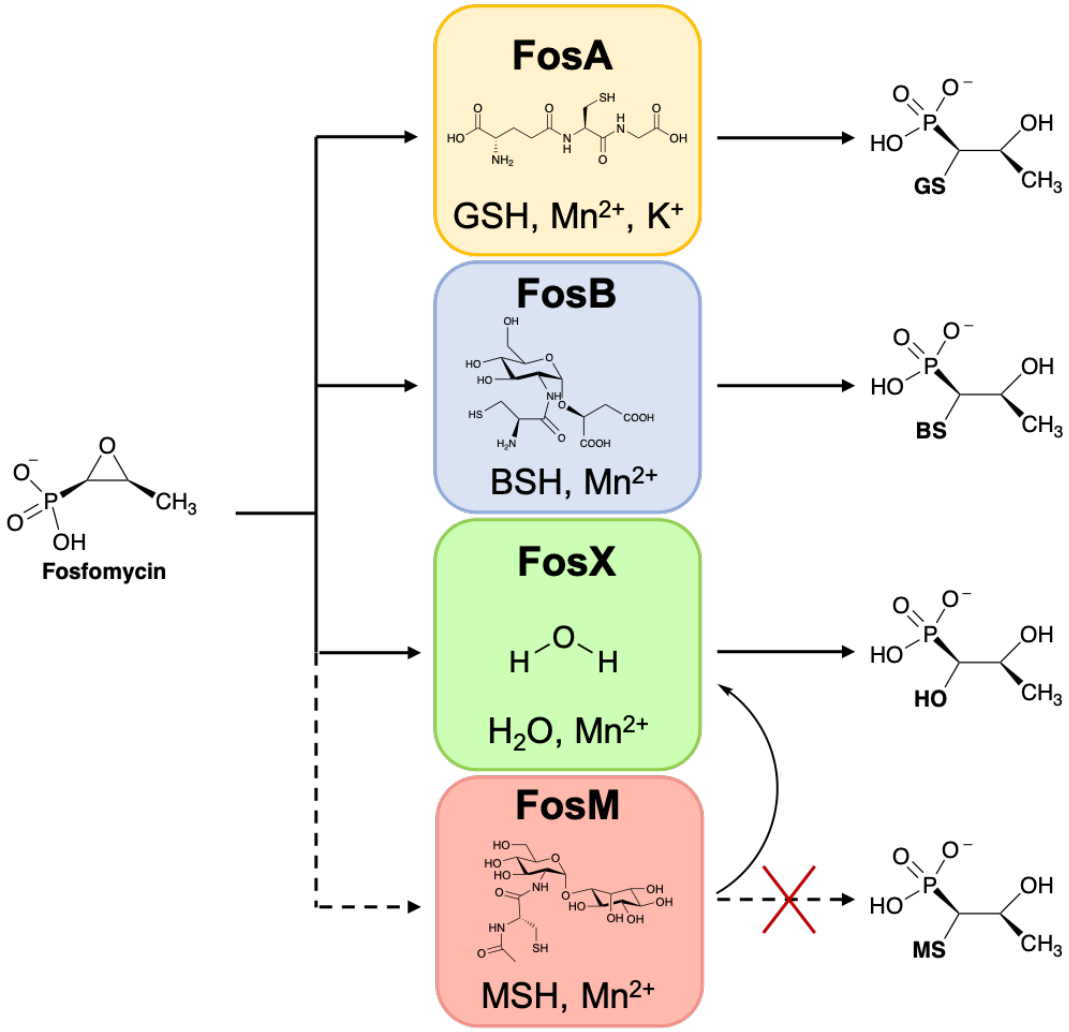
FosA
GSH, Mn2+, K+
FosB
BSH, Mn2+
FosX
H2O, Mn2+
FosM
MSH, Mn2+
Fosfomycin
GS
BS
HO
MS